Syntheses, Kinetics, and Mechanism of Ligand Substitution Reactions of 17-Electron Half-Open Chromocene Carbonyl Complexes

Jian Kun Shen,[†] Jeffrey W. Freeman,[‡] Noel C. Hallinan,[†] Arnold L. Rheingold,*[,§] Atta M. Arif,[‡] Richard D. Ernst,*[,‡] and Fred Basolo*[,†]

Departments of Chemistry, Northwestern University, Evanston, Illinois 60208-3113, University of Utah, Salt Lake City, Utah 84112-1194, and University of Delaware, Newark, Delaware 19716

Received February 25, 1992

Oxidations of monocarbonyl adducts of half-open chromocenes lead to 17-electron adducts such as $Cp(2,4\text{-}C_7H_{11})Cr(CO)^+$ and $Cp^*(3\text{-}C_6H_9)Cr(CO)^+$. X-ray diffraction studies have revealed that in both cases the open dienyl ligands are present in the usual U-shaped conformations. The former, as a CH_3CN solvate of the iodide salt, crystallizes in the monoclinic space group $C2$ with a = 14.593 (3) Å, b = 9.390 (2) Å, c = 13.300 (2) Å, β = 114.91 (2)°, and V = 1652.9 Å^3 for Z = 4. Final discrepancy indices of R = 0.054 and R_w = 0.051 were obtained for 1197 unique, observed reflections. The latter crystallizes in the orthorhombic space group *Pnma* with a = 21.351 (8) Å, b = 8.598 (2) Å, c = 9.763 (4) Å, and V = 1792.2 Å^3 for Z = 4. Final discrepancy indices of R = 0.048 and R_w = 0.050 were obtained for 1074 unique, observed data. Unlike related neutral vanadium and chromium complexes, these cations do not undergo CO exchange reactions readily. However, phosphines readily add to the open dienyl ligands, leading to species such as $Cp^*(1\text{-}PMe_2Ph\text{-}\eta^4\text{-}3\text{-}C_6H_9)Cr(CO)^+$, whose structure was confirmed by a diffraction study of the BF_4^- salt. The compound crystallizes in the orthorhombic space group $Pca2_1$ with a = 9.152 (6) Å, b = 19.206 (8) Å, c = 15.181 (7) Å, and V = 2668.6 Å^3 for Z = 4. Final discrepancy indices of R = 0.066 and R_w = 0.086 were obtained for 1916 unique, observed data. The open dienyl ligands in these as well as the neutral 18-electron complexes are susceptible to loss in the presence of an excess of additional ligands. Through such reactions one may readily isolate $[CpCr(CN\text{-}t\text{-}C_4H_9)_4]^+[BF_4]^-\cdot THF$, $[CpCr(CN\text{-}t\text{-}C_4H_9)_4]^+[CpCr(CO)_3]^-$, $[CpCr(DMPE)(CO)_2]^+[CpCr(CO)_3]^-$, and $[CpCr(CN\text{-}t\text{-}C_4H_9)_3]_2$. Structures of the first two complexes have been determined and found to posses essentially identical cations. For the former, the crystals are triclinic, space group $P\bar{1}$, with a = 10.346 (6) Å, b = 11.832 (8) Å, c = 15.615 (10) Å, α = 78.92 (6)°, β = 72.03 (4)°, γ = 88.85 (4)° and V = 1783 Å^3 for Z = 2. Final discrepancy indices of R = 0.077 and R_w = 0.077 were obtained for 3320 unique, observed reflections. For the latter, the crystals are orthorhombic, space group *Pnma*, with a = 19.785 (4) Å, b = 11.837 (2) Å, c = 15.515 (3) Å, and V = 3633.5 Å^3 for Z = 4. Final discrepancy indices of R = 0.103 and R_w = 0.120 were obtained for 2358 unique, observed reflections. Kinetic studies of CO substitution of $[(Cp)(3\text{-}C_6H_9)Cr(CO)]^+[BF_4]^-$ with an excess of isocyanides or PPh_3 afford a second-order rate law. This and the activation parameters ($\Delta H^\ddagger$ = 16.6 ± 0.2 kcal/mol and $\Delta S^\ddagger$ = −22.6 ± 0.6 cal/(mol·K) for *t*-BuNC) suggest an associative mechanism for the CO substitution reaction. The cationic complex reacts more slowly than does its neutral isoelectronic 17-electron vanadium compound. ESR measurements show that the unpaired electron spin density on Cr is about twice that on V in these two complexes. The retarded rate for CO substitution of the cationic chromium complex compared with that of the vanadium compound may be rationalized in terms of higher electron spin density and a more crowded coordination sphere for Cr, making it more difficult for the nucleophile to attack the half-filled molecular orbital on Cr than on V.

Introduction

Earlier kinetic studies[1] on 17-electron organometallic complexes have shown that they undergo rapid associative ligand substitution compared to analogous 18-electron complexes. This enhanced associative substitution lability of 17-electron complexes was attributed to a more facile nucleophilic attack on the partially occupied metal orbital in 17-electron complexes compared to that on the filled orbital in 18-electron complexes.[1-3] More recently, it has been shown that the 17-electron open and closed vanadocenes react by both associative and dissociative pathways.[4,5] An interesting observation is that $(Pdl)_2VCO$ complexes (Pdl = C_5H_7 or substituted pentadienyl ligand) are less reactive in associative substitution than is Cp_2VCO, although Pdl ligands generally have greater electron-withdrawing ability than does the Cp ligand. This was rationalized[4] in terms of the rigid $(Pdl)_2V$ geometries and reduced spin delocalization making the metal center less susceptible to nucleophilic attack.

Our studies on half-open chromocene carbonyl complexes show they undergo CO exchange predominantly by a dissociative mechanism,[6] a normal behavior of 18-electron complexes. However, these complexes have an unusual η^5(S)-coordinated Pdl, which is different from η^5 (U)-Pdl observed in 16-electron chromium and in 17-electron vanadium carbonyl complexes. We found that these 18-electron half-open chromocene carbonyls were easily oxidized by $NOBF_4$ to the analogous 17-electron complexes. This provides an opportunity for comparing their structures and reactivities with those of analogous 18-electron

[†] Northwestern University.
[‡] University of Utah.
[§] University of Delaware.

(1) (a) McCullen, S. B.; Walker, H. W.; Brown, T. J. *J. Am. Chem. Soc.* 1982, *104*, 4007. (b) Fox, A.; Malito, J.; Poë, A. J. *J. Chem. Soc., Chem. Commun.* 1981, 1052. (c) Zielman, P. M.; Amatore, C.; Kochi, J. K. *J. Am. Chem. Soc.* 1984, *106*, 3771. (d) Hershberger, J. W.; Klinger, R. J.; Kochi, J. K. *J. Am. Chem. Soc.* 1983, *105*, 61. (e) Herrinton, T. R.; Brown, T. L. *J. Am. Chem. Soc.* 1985, *107*, 5700. (f) Shi, Q. Z.; Richmond, T. G.; Trogler, W. C.; Basolo, F. *J. Am. Chem. Soc.* 1984, *106*, 71. (g) Trogler, W. C., Ed. *Organometallic Radical Processes*; Elsevier: Amsterdam. 1990, and references therein.
(2) Harlow, R. L.; McKinney, R. J.; Whitney, J. F. *Organometallics* 1983, *2*, 1839.
(3) Narayanan, B. A.; Kochi, J. K. *J. Organomet. Chem.* 1984, *272*, C49.
(4) Kowaleski, R. W.; Basolo, F.; Trogler, W. C.; Gedridge, R. W.; Newbound, T. D.; Ernst, R. D. *J. Am. Chem. Soc.* 1987, *109*, 4860.
(5) Hallinan, N. C.; Morelli, G.; Basolo, F. *J. Am. Chem. Soc.* 1988, *110*. 6585.
(6) Freeman, J. W.; Hallinan, N. C.; Arif, A. M.; Gedridge, R. W.; Ernst, R. D.; Basolo, F. *J. Am. Chem. Soc.* 1991, *113*, 6509.

0276-7333/92/2311-3215$03.00/0

complexes. The higher oxidation state of the metal atom in these complexes makes them ideal candidates to examine spin localization and steric effects on rates of CO substitution reactions.

Experimental Section

General Procedures. The half-open chromocenes are very air-sensitive, and sometimes pyrophoric. Their ligand adducts are slightly to somewhat air-sensitive. All compounds were therefore prepared, handled, and stored under nitrogen in a glovebox, while solutions were generally manipulated on a high-vacuum or Schlenk line under N_2, Ar, or CO. Hydrocarbon and ethereal solvents were predried and distilled under N_2 from Na/benzophenone prior to use. NMR spectral data were obtained on a Varian XL-300 spectrometer, IR spectral data were obtained on a Perkin-Elmer Model 298 spectrophotometer, and mass spectra were recorded on a VG Micromass 7070 double-focusing mass analyzer with a VG Data System 2000 at an ionizing potential of 17 eV. Magnetic susceptibilities were determined by the Evans method using solution samples.[7] Elemental analyses were obtained from Desert Analytics (Tucson, AZ) and the Analytische Laboratorien (Gummersbach, Germany).

The various dienes, phosphines, and phosphites were either purchased or prepared by published procedures.[8] Manipulations of $CrCl_3(THF)_3$,[9] dienyl anions,[10] and the various half-open chromocenes[6] were performed on a Schlenk line under an atmosphere of prepurified nitrogen. Unless otherwise stated, the reactions were carried out in 250-mL three-neck round-bottom flasks equipped with magnetic stirring bars and, when necessary, either pressure-equalizing dropping funnels or solid addition funnels. Solvent transfers were carried out by syringe. When refluxing of the mixture was required, a water-cooled reflux condenser with a nitrogen inlet was attached. Filtrations utilized coarse glass frits covered with a small amount of Celite.

$[Cp(2,4\text{-}Me_2Pdl)CrCO]^+[BF_4]^-$. A 0.50-g (2.1-mmol) sample of Cp(2,4-Me_2Pdl)Cr(CO) dissolved in 20 mL of CH_2Cl_2 was cooled to −78 °C in an ice bath. A 0.24-g (2.1-mmol) portion of $[NO][BF_4]$ was slowly added to the solution, and the resulting mixture was slowly allowed to come to ambient temperature. The solvent was then removed in vacuo and the residue extracted with 3 × 10 mL of acetone. The acetone solutions often acquire a dark green color. The extracts were filtered, concentrated to ca. 5 mL, and cooled to −80 °C. The product formed orange crystals which were isolated and dried under vacuum. The product was purified by recrystallization from acetone (yield 25% (0.17 g)). IR data (Nujol mull): 3115 (sh), 3110 (m), 2022 (s), 1998 (s), 1493 (sh), 1422 (m), 1283 (m), 1117 (sh), 1095 (sh), 1050 (s, br), 1047 (sh), 1033 (sh), 997 (sh), 947 (w), 927 (w), 872 (m), 847 (m), 833 (w) cm^{-1}. FT-IR (acetonitrile): 2018.5 cm^{-1}. Magnetic susceptibility: $\mu = 2.0\ \mu_B$. Anal. Calcd for $C_{13}H_{16}BCrF_4O$: C, 47.74; H, 4.93. Found: C, 47.04; H, 4.89.

$[Cp(2,4\text{-}Me_2Pdl)CrO]^+I^-\cdot CH_3CN$. A 1.60-g (6.7-mmol) sample of Cp(2,4-Me_2Pdl)Cr(CO) dissolved in 50 mL of ether was cooled to −78 °C. A solution of 0.85 g (3.3 mmol) of I_2 in 25 mL of ether was added dropwise to the solution. The reagents instantly reacted to form an orange-brown precipitate, while the solution remained yellow. The reaction mixture was then warmed to room temperature and the solvent removed in vacuo. The residue was extracted with 3 × 15 mL of hexane to remove the unreacted starting material, which was recovered in 47% yield by crystallization from hexane at −80 °C. The residue was then extracted with 3 × 25 mL of CH_3CN, and the extracts were filtered. The filtrate was concentrated to 30 mL and cooled to −30 °C. The product formed orange crystals that were isolated by syringing off the green supernatnant. The product could be purified by recrystallization from CH_3CN (yield 36% (0.52 g) based on recovered starting material; mp 83–85 °C dec). The green supernatant was concentrated to dryness, yielding a dark green solid that was soluble in THF and was later identified as $(C_5H_5)CrI_2(THF)$. IR data (Nujol mull): 3095 (w), 3040 (sh), 2245 (w), 2000 (s, br), 1413 (w), 1040 (w), 1017 (m), 980 (w), 947 (m), 873 (w), 855 (m), 843 (m), 835 (w) cm^{-1}. FT-IR (acetonitrile): 2017.5 cm^{-1}. Magnetic susceptibility: $\mu = 2.0\ \mu_B$. Anal. Calcd for $C_{15}H_{19}CrINO$: C, 44.13; H, 4.69. Found: C, 43.90; H, 4.67.

$[Cp^*(3\text{-}MePdl)CrCO]^+[BF_4]^-$. This compound was prepared by the same route used to prepare $[Cp(2,4\text{-}Me_2\text{-}Pdl)CrCO]^+[BF_4]^-$ (via the reaction with $[NO][BF_4]$) and was crystallized from acetone/ether (yield 50%; mp 130–140 °C dec). X-ray-quality crystals were grown by gaseous diffusion of ether into an acetone solution of the cation and were orange. IR data (Nujol mull): 3880 (w), 3090 (m), 3035 (sh), 2500 (w), 1955 (s, br), 1910 (sh), 1515 (sh), 1492 (m, br), 1402 (w), 1392 (m), 1367 (m), 1283 (m), 1247 (m), 1219 (m), 1163 (m, br), 1095 (s, br), 1075 (sh), 1067 (sh), 1045 (s, br), 1025 (sh), 963 (w), 940 (m), 805 (m), 622 (m) cm^{-1}. FT-IR (acetonitrile): 1990.5 cm^{-1}. Anal. Calcd for $C_{17}H_{24}BCrF_4O$: C, 53.29; H, 6.31. Found: C, 53.65; H, 6.86.

$[Cp^*(1\text{-}PMe_2Ph\text{-}3\text{-}Me\text{-}Pdl)CrCO]BF_4$. A solution of PMe_2Ph in 1,2-dichloroethane was added to a $[Cp^*(3\text{-}MePdl)CrCO]^+[BF_4]^-$ solution in 1,2-dichloroethane. The reaction was followed with an IR spectrophotometer. The absorbance at 1995 cm^{-1} due to the reactant decreased as the band at 1907 cm^{-1} increased. When an equal amount of PMe_2Ph had been added and all the reactant converted to the product, the solvent was removed under vacuum. The residue was washed with pentane and then with toluene. The red-brown solid left was recrystallized from THF/pentane. The structure of this compound was determined by X-ray diffraction (Figure 6).

A similar reaction of $[Cp(2,4\text{-}Me_2Pdl)CrCO]^+[BF_4]^-$ with PMe_2Ph led to a green solid product having ν_{CO} at 1915 cm^{-1} in 1,2-dichloroethane. Analytical data best fit the mixed-valence formulation $[Cp(1\text{-}PMe_2Ph\text{-}2,4\text{-}Me_2Pdl)CrCO]_2Cl(BF_4)_2$, but a definitive assignment must await a single-crystal structural determination. Anal. Calcd for $C_{42}H_{54}B_2Cr_2F_8O_2P_2Cl$: C, 52.22; H, 5.60; P, 6.42; Cl, 3.67. Found: C, 51.96; H, 5.56; P, 6.35; Cl, 3.49.

$[CpCr(CN\text{-}t\text{-}Bu)_4](THF)BF_4$. To a solution of $[Cp(2,4\text{-}Me_2\text{-}Pdl)CrCO]BF_4$ (80 mg) in 10 mL of acetone was added *t*-BuNC (0.3 mL). The reaction mixture was allowed to stand at room temperature for 30 h, and the cloudy solution was then filtered. Acetone was removed under vacuum, and the solid residue was recrystallized in acetone/THF/toluene (1, 5, and 7 mL, respectively) mixed solvent. The red columnlike crystals obtained were washed with pentane and dried at room temperature under a flow of N_2 gas (70 mg, yield 63%). The molecular structure of the product was determined with a Nicolet P$\bar{1}$ autodiffractometer. Anal. Calcd for $C_{29}H_{49}N_4BCrF_4$: C, 57.24; H, 8.06; N, 9.21. Found: C, 57.34; H, 7.98; N, 9.10. IR (acetone): 2156.3 (m), 2098.3 (s), 2057.5 (sh) cm^{-1}. ^1H NMR (CD_2Cl_2): δ 1.49 (s, 36 H), 1.82 (b, 4 H), 3.68 (b, 4 H), 4.52 (b, 5 H).

Reaction of $[Cp(2,4\text{-}Me_2Pdl)CrCO]^+[BF_4]^-$ with $PhCH_2NC$. To an acetone solution (10 mL) containing $[Cp(2,4\text{-}Me_2Pdl)CrCO]^+[BF_4]^-$ (100 mg) was added $PhCH_2NC$ (0.3 mL). The reaction mixture then stood at room temperature for 2 days, during which time the IR band at 2017 cm^{-1} due to CO of the parent compound completely disappeared and two new bands at 2113 (m) and 2172 (s) cm^{-1} observed. The cloudy solution was filtered, and acetone was removed under vacuum. The remaining residue was a deep red oil, which was washed with THF/toluene (1/5; 3 × 10 mL) solvent. The oily product had a single ESR peak at $g = 2.000$ in THF solution at room temperature.

Attempts were made to reduce the compound with magnesium mesh and sodium naphthalenide (Nph). Magnesium mesh was added to a THF solution containing the product, and the mixture was stirred at room temperature for 2 days. The solution changed color from red to green-yellow. The IR spectrum of this solution showed that part of the product decomposed and the 18-electron compound $Cp(2,4\text{-}Me_2Pdl)Cr(CNCH_2Ph)_2$[6] was not formed. A solution of NaNph in THF was slowly added to an equivalent amount of $[Cp(2,4\text{-}Me_2Pdl)Cr(CNCH_2Ph)_2]^+[BF_4]^-$ in solution at −78 °C. An aliquot of the reaction mixture showed no IR band in the region 2000–2400 cm^{-1}. No further attempt was made to

(7) Evans, D. F. *J. Chem. Soc.* **1959**, 2003.

(8) (a) Jitkow, O. N.; Bogert, M. T. *J. Am. Chem. Soc.* **1941**, *63*, 1979. (b) Jutzi, P.; Kohl, F. X. *Organomet. Synth.* **1986**, *3*, 489. (c) Heitsch, C. W.; Verkade, J. G. *Inorg. Chem.* **1962**, *1*, 451. (d) Frajerman, C.; Meunier, B. *Inorg. Synth.* **1983**, *22*, 133.

(9) Collman, J. P.; Kittleman, E. T. *Inorg. Synth.* **1966**, *8*, 150. Vavoulis, A.; Austin, T. E.; Tyree, S. Y. *Inorg. Synth.* **1960**, *6*, 129.

(10) (a) Wilson, D. R.; Ernst, R. D. *Organomet. Synth.* **1986**, *3*, 136. (b) Yasuda, H.; Nishi, T.; Lee, K.; Nakamura, A. *Organometallics* **1983**, *2*, 21.

Table I. Summary of X-ray Data Collection Parameters for $Cp(2,4\text{-}C_7H_{11})Cr(CO)^+I^-\cdot CH_3CN$ (A), $[Cp^*(3\text{-}C_6H_9)Cr(CO)]^+[BF_4]^-$ (B), $[Cp^*(1\text{-}PMe_2Ph\text{-}3\text{-}C_6H_9)CrCO]^+[BF_4]^-$ (C), $CpCr(CN\text{-}t\text{-}C_4H_9)_4^+[BF_4]^-\cdot THF$ (D), and $CpCr(CN\text{-}t\text{-}C_4H_9)_4^+CpCr(CO)_3^-$ (E)

	A	B	C	D	E
formula	$CrC_{15}H_{19}NOI$	$CrC_{17}H_{24}OBF_4$	$CrC_{25}H_{35}OBF_4P$	$CrC_{29}H_{49}N_4OBF_4$	$Cr_2C_{33}H_{46}N_4O_3$
mol wt	408.22	383.18	521.30	608.45	650.75
space group	*C*2	*Pnma*	$Pca2_1$	*Pnma*	$P\bar{1}$
a, Å	14.593 (3)	21.351 (8)	9.152 (6)	19.785 (4)	10.346 (6)
b, Å	9.390 (2)	8.598 (2)	19.206 (8)	11.837 (2)	11.832 (8)
c, Å	13.300 (2)	9.763 (4)	15.181 (3)	15.515 (3)	15.615 (10)
α, deg	90	90	90	90	78.92 (6)
β, deg	114.91 (2)	90	90	90	72.03 (4)
γ, deg	90	90	90	90	88.85 (4)
V, Å^3	1653	1792.2	2668.6	3633.5 (12)	1783 (2)
Z	4	4	4	4	2
cryst dimens, mm	0.17 × 0.35 × 0.42	0.30 × 0.28 × 0.15	0.08 × 0.38 × 0.48	0.32 × 0.32 × 0.38	0.10 × 0.36 × 0.41
D(calcd), g cm^{-3}	1.64	1.42	1.30	1.11	1.21
μ(Mo Kα), cm^{-1}	23.9	6.60	5.23	3.50	6.28
temp, K	289	289	297	297	297
λ, Å	0.710 73	0.710 73	0.710 73	0.710 73	0.710 73
2θ scan range, deg	2.5–45	3–48	4–45	4–45	4–48
data collected	$\pm h,+k,+l$	$+h,+k,+l$	$+h,+k,+l$	$+h,+k,+l$	$\pm h,\pm k,+l$
no. of unique obsd data	1197	1074	1916	2358	3320
R(*F*)	0.054	0.048	0.066	0.103	0.077
$R_w(F)$	0.051	0.050	0.086	0.120	0.077
$\Delta(\rho)$, e Å^{-3}	1.84	0.76	0.76	0.74	0.94

characterize the products of these reactions with Mg and with NaNph.

$[(C_5H_5)Cr(CN\text{-}t\text{-}Bu)_4]^+[(C_5H_5)Cr(CO)_3]^-$. A 0.6–mL (5.3-mmol) sample of *tert*-butyl isocyanide was added to 0.40 g (2.2 mmol) of $(C_5H_5)(C_5H_7)Cr$ in 20 mL of hexane, and the resulting orange solution was placed into a Fischer–Porter pressure tube under a CO atmosphere. The CO pressure was increased to ca. 5 atm and the tube heated to 70 °C for 2 days (the reaction was initially carried out at 1 atm of CO and at room temperature, but it required 1 week of reaction time and the yield of product was less). The orange-yellow product precipitated out of solution during this time. The excess CO was then vented and the product collected on a frit. The product was then washed with 2 × 10 mL of hexane and extracted into 30 mL of acetone. The filtrate was concentrated to 15 mL and cooled to −80 °C. The orange crystals (mp 162–167 °C dec) were isolated by syringing off the supernatant and dried under vacuum: yield 43% (0.31 g). ^{1}H NMR (acetone-d_6, ambient temperature): δ 4.68 (s, 5 H, C_5H_5), 4.31 (s, 5 H, C_5H_5), 1.54 (s, 36 H, $C(CH_3)_3$). ^{13}C NMR (acetonitrile-d_3, ambient temperature δ 246.80 (s, 3 C, CO), 186.78 (s, 4 C, *C*NR), 88.24 (d of qn, 5 C, C_5H_5, J = 177, 7 Hz), 81.99 (d of qn, 5 C, C_5H_5, J = 172, 7 Hz), 58.91 (s, 4 C, $C(CH_3)_3$), 31.06 (q, 36 C, $C(CH_3)_3$, J = 127 Hz). IR (Nujol mull): 3780 (w), 3645 (w), 3620 (w), 3115 (w), 3100 (w), 2150 9), 2095 (s, br), 2045 (sh), 1890 (s), 1770 (s, br), 1367 (sh), 1305 (w), 1260 (w), 1233 (m), 1195 (m, br), 1110 (m), 1040 (w), 1005 (w), 833 (w), 787 (w), 733 (m), 692 (m), 650 (m), 642 (sh) cm^{-1}. FT-IR (acetonitrile): 2155.4, 2006.5, 2063 (sh), 1893.1, 1774.5 cm^{-1}. Anal. Calcd for $C_{33}H_{46}Cr_2N_4O_3$: C, 60.91; H, 7.12; N, 8.61. Found: C, 60.85; H, 7.01; N, 8.71.

$[(C_5H_5)Cr(DMPE)(CO)_2]^+[(C_5H_5)Cr(CO)_3]^-$. To a 0.40-g (2.2-mmol) sample of $(C_5H_5)(C_5H_7)Cr$ in 10 mL of THF was added 0.40 mL (2.4 mmol) of DMPE to form a DMPE adduct. The solution was stirred under 1 atm of CO for 30 h, resulting in the formation of a red-yellow solution. The yellow product precipitated out of solution after the addition of 20 mL of hexane. The solid was collected on a frit and extracted into 25 mL of acetone. The filtrate was concentrated to ca. 10 mL, and 5 mL of ether was added. The filtrate was then cooled to −30 °C, resulting in the formation of yellow crystals (mp 207–215 °C dec), which were isolated and dried under vacuum: yield 35% (0.20 g). ^{1}H NMR (acetonitrile-d_3, ambient temperature): δ 5.01 (t, 5 H, C_5H_5, J_{P-H} = 1.2 Hz), 4.41 (s, 5 H, C_5H_5), 1.81 (apparent t, 6 H, DMPE CH_3, J_{P-H} = 5.6 Hz), 1.70 (broad s, 2 H, DMPE CH_2), 1.51 (apparent t, 6 H, DMPE CH_3, J_{P-H} = 5.1 Hz), 1.20 (broad s, 2 H, DMPE CH_2). ^{13}C NMR (acetonitrile-d_3, ambient temperature): δ 247.04 (s, 3 C, CO), 246.23 (d, 2 C, CO, J_{P-C} = 60.5 Hz), 90.29 (d of qn, 5 C, C_5H_5, J = 179.3, 7 Hz), 82.76 (d of qn, 5 C, C_5H_5, J = 171.7, 7 Hz), 29.68 (m, J_{P-C} = 20 Hz), 19.63 (m, DMPE). IR (Nujol mull): 3810 (w), 3630 (w), 3610 (w), 3510 (w), 3480 (w), 3120 (m), 3085 (m), 1950 (s), 1893 (s), 1875 (s), 1855, (sh), 1780 (s, br), 1740 (s, br), 1720 (sh), 1430 (m), 1410 (m), 1307 (m), 1292 (m), 1255 (w), 1228 (w), 1117 (w), 1107 (w), 1087 (m), 1067 (m), 1012 (m), 1000 (m), 950 (sh), 937 (s), 925 (s), 895 (w), 873 (w), 860 (w), 842 (m), 807 (sh), 797 (m), 742 (m), 690 (m), 648 (s, br), 640 (sh), 605 (m) cm^{-1}. FT-IR (acetonitrile): 1965.5 (m), 1904.0 (sh), 1893.1 (s), 1774.5 (vs) cm^{-1}. Anal. Calcd for $C_{21}H_{26}Cr_2O_5P_2$: C, 48.10; H, 5.00. Found: C, 47.97; H, 5.27.

$[(C_5H_5)Cr(t\text{-}BuNC)_3]_2$. A 1.0-mL (8.8-mmol) sample of *tert*-butyl isocyanide was added to 0.50 g (2.7 mmol) of $(C_5H_5)(C_5H_7)Cr$ in 25 mL of hexane. The orange-red solution that formed was refluxed for 2 days, which resulted in the formation of a deep red solution and a dark precipitate. The precipitate was collected on a frit, washed with 2 × 10 mL of hexane, and extracted into 30 mL of CH_3CN. The green filtrate was concentrated to ca. 15 mL, and 10 mL of ether was added. The filtrate was then cooled to −30 °C. The product formed green microcrystals that were isolated and dried under vacuum (yield 35%, 0.35 g; mp 176 °C dec). ^{1}H NMR (acetonitrile-d_3, ambient temperature): δ 4.58 (s, 5 H, C_5H_5), 1.47 (s, 27 H, t-C_4H_9). ^{13}C NMR (acetonitrile-d_3, ambient temperature): δ 183.65 (s, 3 C, CNR), 86.74 (d, 5 C, C_5H_5, J = 176.1 Hz), 57.17 (s, 3 C, $C(CH_3)_3$), 29.80 (q, 9 C, $C(CH_3)_3$, J = 128.4 Hz). IR (Nujol mull): 3080 (w), 2140 (s), 2085 (s), 2040 (s), 1365 (sh), 1269 (m), 1231 (s), 1190 (s, br), 1020 (m), 1011 (m), 863 (w), 842 (sh), 837 (m), 832 (m), 807 (s), 731 (s) cm^{-1}.

Kinetic Studies. Kinetic data were obtained by following the decrease of ν_{CO} bands of the reactants with a Nicolet 5PC-FT-IR spectrophotometer using a 0.2-mm NaCl IR cell. The CO substitution reactions of $[Cp(Pdl)CrCO]^+[BF_4]^-$ with RNC and PR_3 (eqs 4 and 7) were studied in acetone and dichloroethane, respectively, under conditions having concentrations of phosphorus ligands at least 10 times greater than that of carbonyl complexes. The dissociation of CO from $[Cp(PMe_2Ph\text{-}Pdl)CrCO]^+[BF_4]^-$ (eq 10) was examined in THF without any phosphine ligand. Constant temperatures (±0.1 °C) were maintained with a Haake Model F circulator. Solutions for ligand substitution studies were kept in the dark. Plots of ln *A* vs time for the disappearance of reactants were linear over 2 half-lives (correlation coefficients >0.99).

X-ray Structural Studies. Single crystals of each of the described compounds were obtained by slow cooling of their concentrated solutions in the solvents mentioned in their preparations. Pertinent parameters relating to data collections and refinements are provided in Table I. Data for **$[Cp(2,4\text{-}C_7H_{11})Cr(CO)]^+I^-\cdot CH_3CN$** and **$[Cp^*(3\text{-}C_6H_9)Cr(CO)]^+[BF_4]^-$** were collected using a Nicolet $P\bar{1}$ autodiffractometer with accompanying software. All calculations employed the Enraf-Nonius SDP programs. Direct methods were used to find the approximate locations of the chromium and iodine (as well as several lighter)

Table II. Positional Parameters for the Non-Hydrogen Atoms of $[Cp^*(3\text{-}C_6H_9)Cr(CO)]^+[BF_4]^-$

atom	x	y	z
Cr	0.08407 (5)	0.25	0.2272 (1)
C(1)	0.0115 (2)	0.4231 (6)	0.2734 (5)
C(2)	0.0486 (2)	0.3960 (6)	0.3891 (5)
C(3)	0.0613 (3)	0.25	0.4520 (7)
C(4)	0.0951 (4)	0.25	0.5868 (7)
C(5)	0.1488 (2)	0.3339 (5)	0.0683 (5)
C(6)	0.1718 (2)	0.3826 (5)	0.1958 (4)
C(7)	0.1870 (3)	0.25	0.2734 (7)
C(8)	0.1356 (3)	0.4359 (8)	−0.0538 (5)
C(9)	0.1840 (3)	0.5495 (6)	0.2348 (6)
C(10)	0.2225 (4)	0.25	0.4065 (8)
C(11)	0.0296 (3)	0.25	0.0788 (8)
O	−0.0034 (3)	0.25	−0.0136 (6)
B	0.1531 (4)	0.75	0.6034 (9)
F(1)	0.1032 (2)	0.75	0.5156 (5)
F(2)	0.1313 (3)	0.75	0.7379 (6)
F(3)	0.1875 (2)	0.6231 (5)	0.5910 (5)

atoms, after which the remaining non-hydrogen atoms were found readily from difference Fourier maps. In subsequent refinements of positional parameters the function $\sum w(|F_o| - |F_c|)$ was minimized. Once the non-hydrogen atom locations had been nearly refined to convergence, difference Fourier maps were used to locate the hydrogen atoms. These atoms were included in their positions but were not refined. All structural solutions and refinements proceeded routinely. Parameters for the latter structure are provided in Tables II and III.

For $[Cp^*(1\text{-}PMe_2Ph\text{-}3\text{-}MePdl)CrCO]^+[BF_4]^-$, photographic data indicated that the crystal possessed *mmm* Laue symmetry; systematic absences determined either of the space groups $Pca2_1$ (noncentrosymmetric) and *Pcam* (centrosymmetric). Initially, the absence of mirror-plane symmetry in the proposed molecule and the statistical distribution of E values suggested that the noncentrosymmetric alternative was correct. The subsequent chemically reasonable and computationally stable refinement in this space group confirmed its choice.

The structure was solved by an autointerpreted Patterson projection. Disorder in the BF_4^- counterion was modeled as a rotational disorder about about the F(2)–B axis. All non-hydrogen atoms were anisotropically refined, and all hydrogen atoms were treated as idealized contributions. An enantiomorphic test based on the refinement of a multiplicative term (1.15 (13)) for $\Delta f'''$ indicated that the reported hand is correct and that the noncentrosymmetric assignment was correct. All computations used programs contained in the SHELXTL program library (version 5.1, G. Sheldrick, Nicolet (Siemens), Madison, WI). Atomic coordinates are given in Table IV, and selected bond distances and angles are given in Table V.

For $[CpCr(CN\text{-}t\text{-}Bu)_4]^+[BF_4]^-\cdot THF$, a large number of specimens of crystals were screened to determine their suitability for a diffraction study. All diffracted weakly and broadly, most likely the result of a minor loss of THF from the crystal lattice and the disorder described below. From photographic evidence, *mmm* Laue symmetry was determined, and systematic absences indicated the space groups $Pn2_1a$ (noncentrosymmetric) and *Pnma* (centrosymmetric). On the basis of the alignment of the crystallographic and molecular mirror planes, the centrosymmetric alternative was chosen, thereby imposing mirror plane symmetry on the molecule. In this space group, the methyl groups of one of the crystallographically unique *tert*-butyl groups (C(5) to C(8)) are rotationally disordered about the N(2)–C(4) axis. Additionally, the molecule of THF located during refinement is severely disordered about the crystallographic mirror plane and an adequate model for the disorder could not be constructed. Similarly, the BF_4^- ion has very high fluorine thermal parameters, indicating that it is also not rigidly fixed in the lattice. No relief of any of these instances of disorder was found in the noncentrosymmetric space group, and all further computations were restricted to *Pnma*. The methyl group disorder could be resolved into two ideally staggered sets of three methyl groups. The occupancies of the sets were refined to nearly equal values, and they were thereafter each fixed at half-occupancy.

No correction for absorption was required; $T(\max)/T(\min) = 1.07$. The structure was solved by direct methods. All non-hydrogen atoms (including the half-occupancy methyl carbon atoms) were refined with anisotropic thermal parameter, and hydrogen atoms were treated as idealized contributions. Parameters for this structure are provided in Tables VI and VII.

A crystal of **$[CpCr(CN(t\text{-}C_4H_9))_4]^+[CpCr(CO)_3]^-$** was mounted on a fine glass fiber with epoxy cement. Both axial photographs and cell reduction programs failed to reveal any crystal symmetry higher than triclinic. The centrosymmetric alternative was initially assumed; this choice was later supported by the chemically reasonable results of refinement. An empirical correction for absorption was applied to the data. The structure was solved by heavy-atom methods. All non-hydrogen atoms were refined with anisotropic thermal parameters, and hydrogen atoms were placed in idealized locations. Several of the methyl group carbon atoms in the *t*-Bu groups have large thermal parameters, revealing the presence of disorder in their rotational positions. Atomic coordinates and relevant bonding parameters are given in Tables VIII and IX.

All computations used the SHELXTL (version 5.1) library of programs (G. Sheldrick, Nicolet (Siemens), Madison, WI).

EPR Spectra. Solutions of the cationic complex in dichloromethane (10^{-3}–10^{-4} M) were prepared in 4-mm quartz tubes fitted with Teflon stopcocks. EPR spectra were recorded at X-band frequency on a Varian E-4 spectrometer at ambient temperature.

Results and Discussion

Syntheses and Structures. The monocarbonyl complexes[6] of half-open chromocenes undergo reversible one-electron oxidations, leading to 17-electron complexes (eqs 1 and 2).

$$Cp(2,4\text{-}Me_2Pdl)CrCO + NO^+ \rightarrow Cp(2,4\text{-}Me_2Pdl)CrCO^+ + NO \quad (1)$$

$$Cp^*(3\text{-}MePdl)CrCO + NO^+ \rightarrow Cp^*(3\text{-}MePdl)CrCO^+ + NO \quad (2)$$

These complexes are notable in that they are rare examples of transition-metal pentadienyl compounds in "higher" oxidation states. They possess one unpaired electron, exhibit typical ESR spectra, and have C–O stretching frequencies more than 100 cm^{-1} higher that those of the neutral species. Due to the paramagnetism

Table III. Bond Distances (Å) and Angles (deg) for $[Cp^*(3\text{-}C_6H_9)Cr(CO)]^+[BF_4]^-$

Bond Distances

Cr–C(1)	2.195 (4)	Cr–C(5)	2.199 (4)	B–F(1)	1.367 (8)	C(5)–C(6)	1.402 (5)
Cr–C(2)	2.156 (4)	Cr–C(6)	2.214 (4)	B–F(2)	1.393 (9)	C(6)–C(7)	1.407 (5)
Cr–C(3)	2.248 (6)	Cr–C(7)	2.244 (5)	B–F(3)	1.320 (5)	C(5)–C(8)	1.506 (6)
Cr–C(11)	1.858 (7)	C(1)–C(2)	1.399 (6)	C(3)–C(4)	1.500 (8)	C(6)–C(9)	1.508 (5)
O–C(11)	1.145 (7)	C(2)–C(3)	1.424 (5)	C(5)–C(5′)	1.442 (8)	C(7)–C(10)	1.505 (8)

Bond Angles

C(1)–C(2)–C(3)	127.1 (4)	C(5′)–C(5)–C(8)	125.6 (2)	Cr–C(11)–O	179.2 (6)
C(2)–C(3)–C(2′)	123.7 (5)	C(6)–C(5)–C(8)	126.4 (4)	F(1)–B–F(2)	109.2 (6)
C(2)–C(3)–C(4)	118.0 (3)	C(5)–C(6)–C(9)	124.7 (4)	F(1)–B–F(3)	112.1 (4)
C(5′)–C(5)–C(6)	107.4 (2)	C(7)–C(6)–C(9)	126.5 (4)	F(2)–B–F(3)	105.8 (5)
C(5)–C(6)–C(7)	108.5 (3)	C(6)–C(7)–C(10)	125.6 (2)	F(3)–B–F(3′)	111.5 (7)
C(6)–C(7)–C(6′)	108.3 (5)				

Table IV. Atomic Coordinates and Equivalent Isotropic Displacement Coefficients for [Cp*(1-PMe$_2$Ph-3-MePdl)CrCO]$^+$[BF$_4$]$^-$

	x	y	z	U, Å^2
Cr	2019 (2)	2500	-317 (2)	38 (1)
N(1)	3105 (5)	827 (10)	393 (8)	77 (3)
N(2)	1156 (6)	876 (10)	773 (8)	77 (3)
B	4747 (19)	2500	8516 (25)	139 (3)
F(1)	4942 (10)	1708 (15)	8090 (12)	341 (3)
F(2)	4126 (9)	2500	8475 (14)	254 (3)
F(3)	5036 (9)	2500	9205 (11)	173 (3)
C(1)	1355 (11)	2500	-1443 (14)	110 (3)
C(2)	1720 (12)	1561 (14)	-1457 (11)	131 (3)
C(3)	2377 (8)	1915 (16)	-1568 (8)	128 (3)
C(4)	1482 (6)	1476 (11)	376 (9)	59 (3)
C(5)	868 (8)	124 (13)	1432 (9)	81 (3)
C(6)	671 (26)	843 (30)	2153 (26)	169 (3)
C(7)	347 (17)	-638 (31)	1051 (24)	132 (3)
C(8)	1480 (17)	-823 (29)	1652 (23)	124 (3)
C(9)	2694 (6)	1467 (11)	152 (7)	56 (3)
C(10)	3632 (7)	60 (13)	621 (9)	78 (3)
C(11)	4217 (8)	796 (16)	956 (12)	126 (3)
C(12)	3854 (9)	-567 (14)	-182 (12)	122 (3)
C(13)	3342 (9)	-787 (15)	1272 (13)	132 (3)
C(6′)	1299 (19)	325 (33)	2164 (22)	127 (3)
C(7′)	109 (14)	541 (29)	1556 (22)	102 (3)
C(8′)	890 (23)	-1145 (25)	1066 (25)	138 (3)

Table V. Selected Bond Distances (Å) and Angles (deg) for [Cp*(1-PMe$_2$Ph-3-Me-Pdl)CrCO]$^+$[BF$_4$]$^-$

(a) Bond Distances

Cr–CNT	1.860 (10)	Cr–C(6)	2.139 (9)
Cr–C(1)	1.817 (11)	C(3)–C(4)	1.38 (2)
Cr–C(3)	2.165 (11)	C(4)–C(5)	1.35 (2)
Cr–C(4)	2.146 (12)	C(5)–C(6)	1.41 (1)
Cr–C(5)	2.108 (10)	C(6)–C(7)	1.54 (1)

Bond Angles

CNT–Cr–C(1)	111.9 (5)	C(4)–C(5)–C(6)	120 (1)
C(3)–C(4)–C(5)	124 (1)	C(5)–C(6)–C(7)	127 (1)

Table VI. Positional Parameters for the Non-Hydrogen Atoms of [CpCr(CN-t-C$_4$H$_9$)$_4$]$^+$[BF$_4$]$^-$•THF

atom	x	y	z
Cr	0.2019 (1)	0.25	-0.0317 (2)
N(1)	0.3105 (5)	0.0827 (10)	0.0393 (8)
N(2)	0.1156 (6)	0.0876 (10)	0.0773 (8)
B	0.4747 (19)	0.25	0.8516 (25)
F(1)	0.4942 (10)	0.1708 (15)	0.8090 (12)
F(2)	0.4126 (9)	0.25	0.8475 (14)
F(3)	0.5036 (9)	0.25	0.9205 (11)
C(1)	0.1355 (11)	0.25	-0.1443 (14)
C(2)	0.1720 (12)	0.1561 (14)	-0.1457 (11)
C(3)	0.2377 (8)	0.1915 (16)	-0.1568 (8)
C(4)	0.1482 (6)	0.1476 (11)	0.0376 (9)
C(5)	0.0868 (8)	0.0124 (13)	0.1432 (9)
C(6)	0.0671 (26)	0.0843 (30)	0.2153 (26)
C(7)	0.0347 (17)	-0.0638 (31)	0.1051 (24)
C(8)	0.1480 (17)	-0.0823 (29)	0.1652 (23)
C(9)	0.2694 (6)	0.1467 (11)	0.0152 (7)
C(10)	0.3632 (7)	0.0060 (13)	0.0621 (9)
C(11)	0.4217 (8)	0.0796 (16)	0.0956 (12)
C(12)	0.3854 (9)	-0.0567 (14)	-0.0182 (12)
C(13)	0.3342 (9)	-0.0787 (15)	0.1272 (13)
C(6′)	0.1299 (19)	0.0325 (33)	0.2164 (22)
C(7′)	0.0109 (14)	0.0541 (29)	0.1556 (22)
C(8′)	0.0890 (23)	-0.1145 (25)	0.1066 (25)
O	0.2842 (23)	0.25	0.2655 (29)
C(15)	0.3633 (26)	0.25	0.3571 (34)
C(16)	0.3150 (26)	0.25	0.4201 (30)
C(17)	0.2882 (20)	0.1557 (24)	0.3405 (23)

of these compounds, X-ray diffraction studies were required to establish the mode of pentadienyl bonding.

Although mono(ligand) adducts of the half-open chromocenes appear invariably to possess η^5-S-pentadienyl coordination,[5] oxidation to 17-electron monocations seems to return the open ligand to the more usual U conformation, as demonstrated by structural results on the Cp(2,4-Me$_2$Pdl)Cr(CO)$^+$ and Cp*(3-MePdl)Cr(CO)$^+$ salts. Unfortunately, an accurate structural result could not be obtained for the former complex as a result of pseudosymmetry and/or disorder, leading to partially overlapping C_5H_5 and 2,4-Me$_2$Pdl images. However, the general result (Figure 1 and supplementary material) did demonstrate that η^5(U)-2,4-Me$_2$Pdl coordination was present, as was an eclipsed conformation (I). In the hope of obtaining more accurate structural data, and of further confirming the

Table VII. Selected Bonding Parameters for [CpCr(CN-t-C$_4$H$_9$)$_4$]$^+$[BF$_4$]$^-$•THF

Bond Distances (Å)

Cr–C(1)	2.186 (21)	Cr–C(4)	1.938 (13)	N(1)–C(10)	1.428 (18)
Cr–C(2)	2.171 (18)	Cr–C(9)	1.951 (13)	N(2)–C(4)	1.141 (18)
Cr–C(3)	2.178 (14)	N(1)–C(9)	1.172 (17)	N(2)–C(5)	1.470 (19)

Bond Angles (deg)

C(4)–Cr–C(4′)	77.4 (8)	C(9)–N(1)–C(10)	175.3 (13)
C(4)–Cr–C(9)	77.1 (5)	C(4)–N(2)–C(5)	166.4 (14)
C(4)–Cr–C(9′)	124.1 (6)	Cr–C(4)–N(2)	178.7 (11)
C(9)–Cr–C(9′)	77.7 (8)	Cr–C(9)–N(1)	176.7 (11)

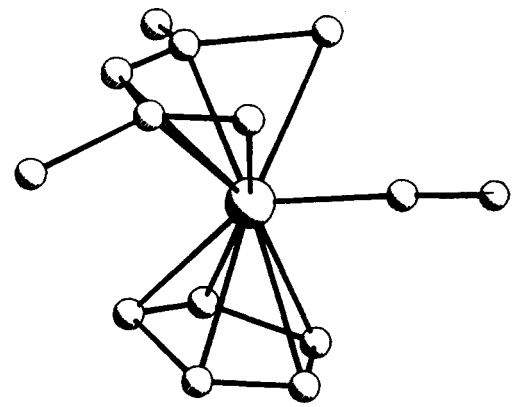

Figure 1. Approximate molecular structure of Cp(2,4-C$_7$H$_{11}$)CrCO$^+$.

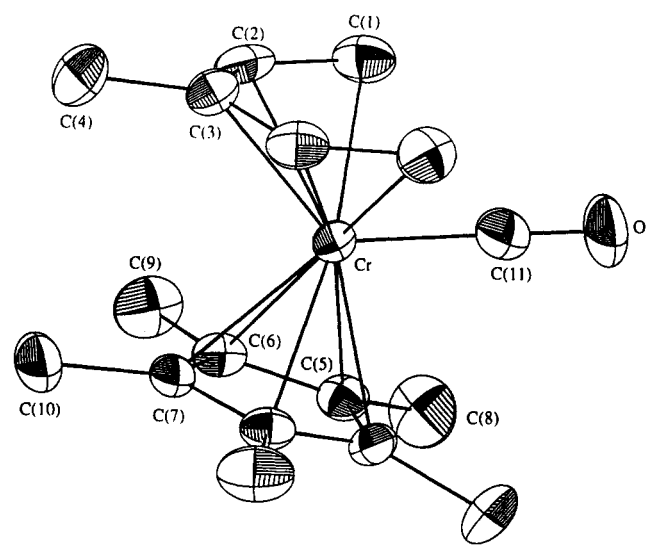

Figure 2. Molecular structure of Cp*(3-C$_6$H$_9$)CrCO$^+$.

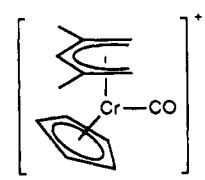

I

Table VIII. Positional Parameters for the Non-Hydrogen Atoms of $[CpCr(CN\text{-}t\text{-}C_4H_9)_4]^+[CpCr(CO)_3]^-$

atom	x	y	z
Cr(1)	0.3836 (1)	0.1921 (1)	0.2455 (1)
Cr(2)	1.1862 (1)	0.7012 (1)	0.1868 (1)
C(1)	0.2418 (8)	0.3006 (7)	0.1939 (6)
C(2)	0.1732 (9)	0.2019 (11)	0.2485 (7)
C(3)	0.2283 (11)	0.1112 (9)	0.2061 (8)
C(4)	0.3303 (10)	0.1584 (8)	0.1270 (6)
C(5)	0.3330 (9)	0.2733 (8)	0.1218 (6)
C(6)	0.3805 (8)	0.7146 (11)	0.2187 (8)
C(7)	1.3746 (11)	0.8053 (10)	0.1391 (14)
C(8)	1.3665 (10)	0.7469 (11)	0.0699 (9)
C(9)	0.3692 (9)	0.6338 (9)	0.1011 (7)
C(10)	1.3776 (9)	0.6209 (10)	0.1872 (8)
C(11)	0.3496 (8)	0.0689 (7)	0.3516 (5)
C(12)	0.2750 (10)	−0.0962 (7)	0.4952 (5)
C(13)	0.3835 (20)	−0.1758 (15)	0.4923 (15)
C(14)	0.1725 (23)	−0.1642 (15)	0.4876 (11)
C(15)	0.2502 (25)	−0.0519 (12)	0.5749 (9)
C(16)	0.3479 (8)	0.2759 (6)	0.3454 (5)
C(17)	0.2562 (9)	0.3813 (7)	0.4805 (5)
C(18)	0.0971 (13)	0.3533 (11)	0.5031 (7)
C(19)	0.2870 (14)	0.3237 (10)	0.5624 (7)
C(20)	0.2728 (18)	0.5076 (9)	0.4551 (9)
C(21)	0.5390 (7)	0.3016 (6)	0.2032 (5)
C(22)	0.7483 (7)	0.4462 (7)	0.1592 (5)
C(23)	0.7160 (9)	0.5132 (9)	0.2342 (7)
C(24)	0.7597 (11)	0.5229 (9)	0.0665 (7)
C(25)	0.8721 (9)	0.3798 (8)	0.1553 (7)
C(26)	0.5384 (8)	0.0956 (6)	0.2056 (5)
C(27)	0.7443 (7)	−0.0322 (6)	0.1510 (5)
C(28)	0.8739 (9)	0.0348 (8)	0.1418 (7)
C(29)	0.7214 (9)	−0.1387 (7)	0.2243 (6)
C(30)	0.7484 (11)	−0.0549 (9)	0.0584 (6)
C(31)	1.0857 (8)	0.7952 (7)	0.2576 (5)
C(32)	1.0796 (8)	0.5780 (7)	0.2585 (5)
C(33)	1.0740 (8)	0.7209 (7)	0.1151 (5)
N(1)	0.3233 (7)	−0.0036 (6)	0.4161 (4)
N(2)	0.3208 (7)	0.3267 (6)	0.4052 (4)
N(3)	0.6336 (7)	0.3654 (6)	0.1794 (4)
N(4)	0.6285 (7)	0.0404 (5)	0.1793 (4)
O(31)	1.0224 (6)	0.8587 (5)	0.3031 (9)
O(32)	1.0124 (6)	0.4999 (5)	0.3057 (4)
O(33)	1.0070 (6)	0.7341 (5)	0.0679 (4)

generality of the η^5(U)-pentadienyl coordination mode in these paramagnetic cations a structural determination was carried out on $[Cp^*(3\text{-Me-Pdl})Cr(CO)]^+[BF_4]^-$, whose greater number of methyl groups was expected to lead to a more ordered structure. This indeed turned out to be the case (Figure 2; Tables II and III), and as for $Cp(2,4\text{-}Me_2Pdl)Cr(CO)^+$, an eclipsed conformation (I) was observed, with crystallographically imposed mirror-plane symmetry. Apparently, eclipsing H–H or CH_3–CH_3 interactions in the two cationic structures are less severe than the H–CO or CH_3–CO repulsions that would ensue in the staggered forms. The average Cr–C distances for the open and closed ligands are similar at 2.190 (3) and 2.214 (3) Å, respectively, and can be seen to be slightly longer than the corresponding averages for the 18-electron isocyanide complex $Cp(\eta^5(S)\text{-}C_5H_7)Cr(CN\text{-}2,6\text{-}(CH_3)_2C_6H_3)$.[6] For both ligands, the longest Cr–C distance involves the carbon atoms (C(3) or C(7)) engaged in the eclipsing interaction. The significance of the eclipsing interactions may also be gauged by the relative tilts of the methyl groups from the ligand planes. As the pentadienyl ligands seem invariably larger than optimal for metal–ligand overlap, significant

Scheme I. Reaction Mechanism

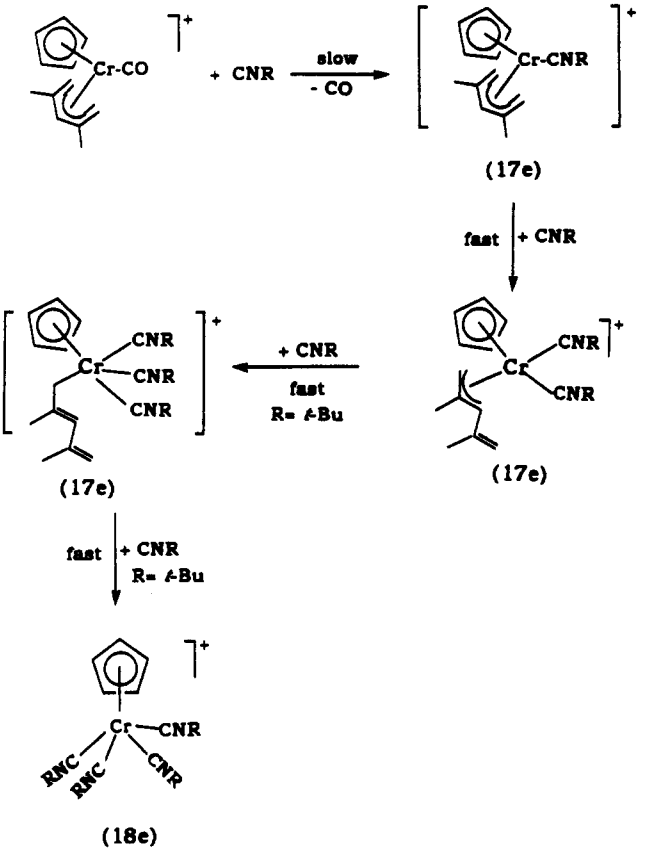

Table IX. Selected Bonding Parameters for $[CpCr(N\text{-}t\text{-}C_4H_9)_3]^+[CpCr(CO)_3]^-$

Bond Distances (Å)

Cr(1)–C(1)	2.169 (9)	Cr(2)–C(6)	2.231 (11)	N(1)–C(11)	1.153 (9)
Cr(1)–C(2)	2.164 (9)	Cr(2)–C(7)	2.172 (11)	N(1)–C(12)	1.448 (9)
Cr(1)–C(3)	2.185 (13)	Cr(2)–C(8)	2.159 (10)	N(2)–C(16)	1.166 (11)
Cr(1)–C(4)	2.194 (11)	Cr(2)–C(9)	2.190 (9)	N(2)–C(17)	1.426 (11)
Cr(1)–C(5)	2.196 (9)	Cr(2)–C(10)	2.180 (10)	N(3)–C(21)	1.168 (10)
Cr(1)–C(11)	1.931 (7)	Cr(2)–C(31)	1.806 (8)	N(3)–C(22)	1.456 (10)
Cr(1)–C(16)	1.943 (8)	Cr(2)–C(32)	1.808 (7)	N(4)–C(26)	1.143 (10)
Cr(1)–C(21)	1.949 (7)	Cr(2)–C(33)	1.830 (9)	N(4)–C(27)	1.466 (10)
Cr(1)–C(26)	1.960 (7)	C(31)–O(31)	1.181 (10)	C(32)–O(32)	1.153 (9)
C(33)–O(33)	1.146 (12)				

Bond Angles (deg)

C(11)–Cr(1)–C(16)	77.8 (3)	Cr(1)–C(11)–N(1)	176.9 (7)
C(11)–Cr(1)–C(21)	124.2 (4)	Cr(1)–C(16)–N(2)	177.1 (7)
C(11)–Cr(1)–C(26)	78.9 (3)	Cr(1)–C(21)–N(3)	178.2 (7)
C(16)–Cr(1)–C(21)	77.9 (3)	Cr(1)–C(26)–N(4)	177.6 (7)
C(16)–Cr(1)–C(26)	126.7 (4)	C(11)–N(1)–C(12)	173.3 (10)
C(21)–Cr(1)–C(26)	76.9 (3)	C(16)–N(2)–C(17)	166.8 (9)
C(31)–Cr(2)–C(32)	90.6 (3)	C(21)–N(3)–C(22)	174.4 (8)
C(31)–Cr(2)–C(33)	90.5 (4)	C(26)–N(4)–C(27)	176.6 (8)
C(32)–Cr(2)–C(33)	89.0 (4)	Cr(2)–C(31)–O(31)	178.4 (7)
Cr(2)–C(32)–O(32)	178.7 (9)	Cr(2)–C(33)–O(33)	178.0 (6)

substituent tilts are generally observed, as indicated in II,

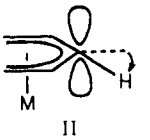

II

apparently in an attempt to point the carbon atom p orbitals toward the metal atom.[11] However, in this case the methyl group (i.e., C(4)) lies significantly out of the ligand plane, by 0.16 Å, *away from* the metal atom, corresponding to tilt of 6.1° in the wrong direction. This may also contribute to the lengthening of the Cr–C(3) bond relative to the other pentadienyl positions. Similarly, C(10) lies further away (0.23 Å) from the cyclopentadienyl ligand plane than do C(8) (0.19 Å) or C(9) (0.09 Å). These observations may readily be attributed to a steric interaction between the eclipsed C(4) and C(10). The fact that C(8) lies nearly as far out of the plane as does C(10) might also be indicative of significant C(8)–CO repulsions. The two ligand planes are tilted from each other by 10.6 (7)° and form angles with the Cr–C(11) vector of 6.1 and 16.7°, respectively. As with the isocyanide complex, the two-electron-donor ligand is therefore seen to be tilted toward the pentadienyl ligand plane. Consistent with other structures,[11] the C(1)–C(2) distance of 1.399 (6) Å is shorter than the C(2)–C(3) distance of 1.424 (5) Å. The presence of the methyl group on C(3) leads to the usual contraction of the C–C–C angle:[11] cf. C(1)–C(2)–C(3) = 127.1 (4)°, while C(2)–C(3)–C(2′) = 123.7 (5)°.

Substitution Reactions of the 17-Electron Complexes with Weak Bases. The reaction of Cp(2,4-Me_2Pdl)CrCO$^+$ with CO in acetonitrile was examined. No CO exchange was observed to occur over a period of 24 h at room temperature. When the solution was heated to 50 °C, the CO peak in the infrared spectrum disappeared and the solution changed color from red to blue. A similar result was observed when the complex was heated under N_2. Kinetic data showed that the rate of disappearance of the CO frequency under an atmosphere of CO (t = 50 °C, k_{obs} = 2.03 × 10^{-4} s^{-1}) was identical with that under N_2 (t = 50 °C, k_{obs} = 2.08 × 10^{-4} s^{-1}).

The reactions of Cp(2,4-Me_2Pdl)CrCO$^+$ with isocyanides were then examined. Since these ligands have strong absorbance bands in the C≡N stretching region (2000–2400 cm^{-1}), the reactions were conveniently monitored by recording the formation of these bands with an IR spectrometer. Changes in the IR spectra for a reaction mixture of the complex and $PhCH_2NC$ in acetone provide kinetic data which show that the rate of reaction is first order in both complex and isocyanide concentrations (eq 3).

$$\frac{d[Cr\text{–}CO]}{dt} = -k_2[CrCO][CNR] \qquad (3)$$

The complex Cp(2,4-Me_2Pdl)CrCO$^+$ reacts with excess $PhCH_2NC$, leading to the apparent incorporation of at least 2 equiv of isocyanide (Figure 3).[12] Unfortunately, the product is a paramagnetic oil, and only limited data could be obtained (ν(C≡N) 2113, 2172 cm^{-1}; ESR singlet, g = 2.000. While these data would be consistent with a formulation such as Cp(η^3-2,4-C_7H_{11})Cr(NCCH_2C$_6$H$_5$)$_2^+$, no direct evidence for the presence of the 2,4-C_7H_{11} ligand could be obtained, and reduction of the product did not proceed readily to Cp(η^3-2,4-C_7H_{11})Cr-(NCCH_2C$_6$H$_5$)$_2$, as

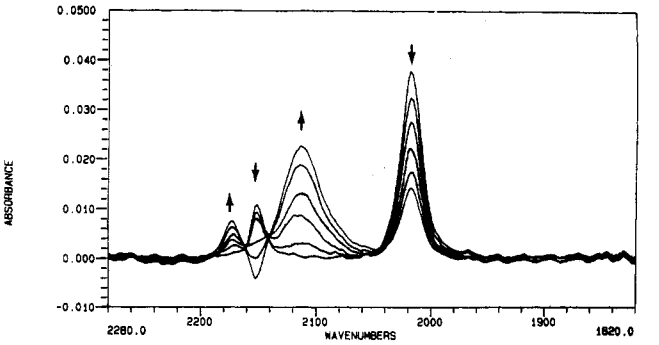

Figure 3. IR spectral changes for reaction of [Cp(2,4-C_7H_{11})-Cr(CO)]$^+$[BF_4]$^-$ with $PhCH_2NC$ at 40 °C.

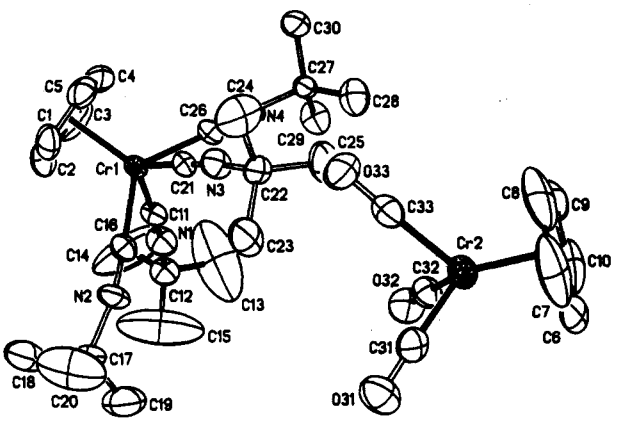

Figure 4. Molecular structure of [CpCr(NC-t-C_4H_9)$_4$]$^+$[CpCr-(CO)$_3$]$^-$.

Table X. Second-Order Rate Constants and Activation Parameters for Reaction 4

T, °C	k, M^{-1} s^{-1}	$\Delta H^‡$, kcal/mol	$\Delta S^‡$, cal/(mol·K)
17.1	2.31 × 10^{-5}	16.6 ± 0.2	−22.6 ● 0.6
29.1	7.61 × 10^{-5}		
40.0	2.03 × 10^{-4}		

would be expected.[6] Hence, the formulation of this material is still unclear.

However, when Cp(2,4-Me_2Pdl)Cr(CO)$^+$ reacts with t-BuNC, the product is [CpCr(CN-t-Bu)$_4$]$^+$ (eq 4). No other intermediate was observed during this reaction. It is

$$Cp(2,4\text{-}Me_2Pdl)Cr(CO)^+ \xrightarrow{CN\text{-}t\text{-}Bu} CpCr(CN\text{-}t\text{-}Bu)_4^+ \qquad (4)$$

believed that the rate-determining first step involves nucleophilic attack of the entering ligand at the metal, which may generate a 19e transition state (Scheme I). A plot of ln k/T vs $1/T$ affords activation parameters (Table X). The relative low $\Delta H^‡$ value and the negative $\Delta S^‡$ value support the suggested associative mechanism for the rate-determining step. In the proposed mechanism (Scheme I), rapid Pdl slippage occurs following the first rate-determining step, allowing for faster subsequent reaction, in accord with the general observation that more basic ligands on a metal facilitate slippage.[13] The open pentadienyl ligand is finally released from the metal center as more t-BuNC enters the coordination sphere. Other examples that a pentadienyl ligand coordinated to the metal is more likely to undergo $\eta^5 \rightarrow \eta^3$ slippage compared with Cp are known,[14] including related reactions for 18e

(11) (a) Ernst, R. D. *Struct. Bonding (Berlin)* **1984**, *57*, 1. (b) Ernst, R. D. *Chem. Rev.* **1988**, *88*, 1255.

(12) There is also a possibility that two products, perhaps isomers, are formed, but this seems less likely.

(13) Freeman, J.; Basolo, F. *Organometallics* **1991**, *10*, 256.

(14) Paz-Sandoval, M. A.; Powell, P.; Drew, M. G. B.; Perutz, R. N. *Organometallics* **1984**, *3*, 1026. Bleeke, J. R.; Peng, W. J. *Organometallics* **1986**, *5*, 635.

complexes (see Experimental Section and eqs 5 and 6).

$$Cp(C_5H_7)Cr(CO) + CO\ (excess) + t\text{-}C_4H_9NC\ (excess) \rightarrow [CpCr(CN\text{-}t\text{-}C_4H_9)_4]^+[CpCr(CO)_3]^- \quad (5)$$

$$Cp(\eta^3\text{-}C_5H_7)Cr(dmpe) + CO\ (excess) \rightarrow [CpCr(dmpe)(CO)_2]^+[CpCr(CO)_3]^- \quad (6)$$

Molybdenum analogs of both products are known, and the nature of $[CpCr(CN\text{-}t\text{-}C_4H_9)]^+[CpCr(CO)_3]^-$ has been confirmed by X-ray diffraction (Figure 4).[15] In the absence of CO, the neutral dimer $[CpCr(CN\text{-}t\text{-}C_4H_9)_3]_2$ may be obtained.

There is no reaction observed between $Cp(2,4\text{-}C_7H_{11})Cr(CO)^+$ and PPh_3 or phosphite ligands after several hours at room temperature. When the 1/1 ligand/complex mixtures were heated in CH_2Cl_2, they slowly changed color from red to green to blue with concomitant decrease and finally disappearance of the CO frequency. ESR spectra of the resulting solutions all show doublets. Relevant g values and coupling constants are in Table XI. These coupling are attributed to the phosphorus atoms of ligands coordinating to the metal atoms, and the similarity to values for the apparent $Cp(Pdl)V(PR_3)$ complexes (ca. 26–45 G) might suggest a reaction such as eq 7. However, the oily nature of these products precluded definitive characterization.

$$Cp(2,4\text{-}Me_2Pdl)Cr(CO)^+ + PR_3 \rightarrow Cp(2,4\text{-}Me_2Pdl)CrPR_3^+ + CO \quad (7)$$

Kinetic studies for the apparent substitution reactions (eq 7) were carried out in 1,2-dichloroethane and under conditions for which the concentrations of the ligands were at least 10 times greater than those of the complexes. The rate constants were obtained by following the decrease of the bands of ν_{CO} of the reactants and included in Table XII.

The reactions of the complexes with PPh_3 proceed predominantly by an associative pathway. In contrast, the rate for the reaction of $Cp^*(3\text{-}MePdl)Cr(CO)^+$ with $P(OPh)_3$ is independent of the ligand concentration (Figure 5). Other results (Table XII) show that the associative rate of CO substitution is faster for $Cp(2,4\text{-}Me_2Pdl)VCO$ than for $[Cp(2,4\text{-}Me_2Pdl)CrCO]^+[BF_4]^-$. Since Cr in the cationic complex is more postiviely charged, one might expect that the cationic complex would be more susceptible to nucleophilic attack. From the results of ESR studies ($A_{iso}(Cr) = 25$ G; $A_{iso}(V) = 58$ G[4]), spin density on the metal atoms can be estimated. It turns out that the single-electron density on Cr in its complex is about 2 times that on the V atom. Since it has been proposed[4,5] that spin localization may retard associative reactions, one might attribute that rate retardation to the greater localization of the single electron on the Cr atom; the higher oxidation state of Cr reduces spin delocalization and destabilizes its reaction transition state.

Although the two complexes have similar coordination environments, it is necessary to consider steric effects on the rate of the reaction. An X-ray structure determination has been obtained for the vanadium complex.[16] The results (Table XIII) show that the cationic chromium complex is more crowded than the vanadium complex. This may in part contribute to the reduced reactivity of the chromium complex toward nucleophilic attack.

Table XI. ESR Parameters for Phosphine Adducts of $Cp(2,4\text{-}C_7H_{11})CrCO^+$

ligand	g^a	g^b	$A(^{31}P)$, G[c]
PMe_2Ph	2.0037	2.008	26
$P(n\text{-}Bu)_3$	2.0031	2.011	24
PCy_3	2.0038	2.008	26
PEt_3	1.9990	1.997	26
$P(OEt)_3$		1.997	33
PPh_3		1.997	24

[a] g value before heating. [b] g value after heating. [c] After heating.

Table XII. Rates of CO Substitution and Ligand Additions for Different Complexes

complex	T, °C	k_1, s^{-1}	k_2, $M^{-1}\ s^{-1}$
$Cp^*(3\text{-}C_6H_9)CrCO^+$	38.4	3.0×10^{-6}	2.0×10^{-4} (PPh_3)[c]
$Cp^*(3\text{-}C_6H_4)CrCO$[a]	37	1.47×10^{-5}	
$Cp^*(1\text{-}PMe_2Ph\text{-}3\text{-}C_6H_9)CrCO^+$	40	3.0×10^{-5} (1.5×10^{-5})[d]	
$Cp(2,4\text{-}C_7H_{11})CrCO^+$	38.4		3.6×10^{-4} (PPh_3)[c] 2.78×10^{-4} ($CNCH_2Ph$)[c] 2.03×10^{-4} (CN-t-Bu)[c]
$Cp(2,4\text{-}C_7H_{11})CrCO$[a]	40	4.04×10^{-4}	
$Cp(2,4\text{-}C_7H_{11})V(CO)$[b]	40	2.3×10^{-6}	1.1×10^{-3} (CO)[c]

[a] Reference 10. [b] Reference 8. [c] Nucleophile in parentheses. [d] Rate constant for reaction in 1 atm of CO.

Table XIII. Comparison of Ligand Parameters (Å) in CpPdlVCO and $Cp^*(3\text{-}C_6H_9)CrCO^+$

	CpPdlVCO	$Cp^*(3\text{-}C_6H_9)CrCO^+$
M–C(CO)	1.916 (3)	1.858 (7)
M–C(Cp)	2.256 (3)	2.214 (3)
M–C(Pdl)	2.213 (2)	2.190 (3)

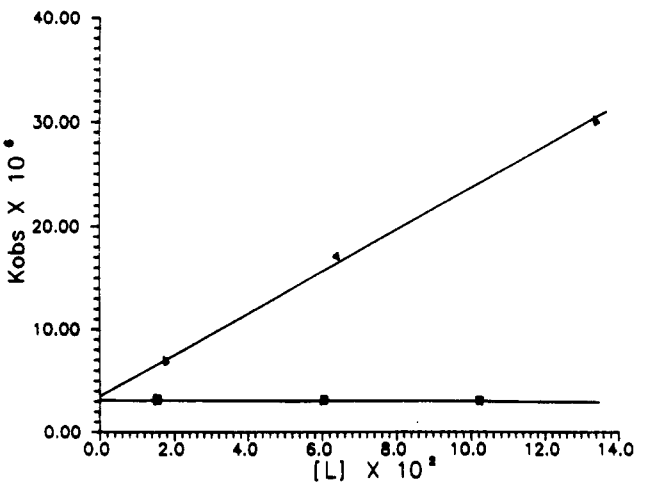

Figure 5. Plot of k_{obsd} vs PR_3 concentrations of PPh_3 (▲) and $P(OPh)_3$ (■) for CO substitution reactions of $Cp^*Cr(3\text{-}C_6H_9)CO^+$.

The results (Table XII) show that the dissociation rate of CO from the cationic complex is about the same as that from the neutral vandium complex and is slower than that of the analogous 18-electron chromium complex. The oxidation of the half-open chromocene carbonyl complexes stabilizes the carbonyl group toward substitution. These observations contrast with the fact that $Cr(CO)_6$[17] is more labile toward substitution than $V(CO)_6$.[1f] $Cr(CO)_6^+$ has only been characterized at −80 °C by ESR spectroscopy, and there is not much information available regarding its

(15) Additional structural details for the isocyanide complexes are presented in the supplementary material.
(16) Gedridge, R. W.; Rheingold, A. L.; Ernst, R. D. Unpublished results.
(17) (a) Bagchi, R. N.; Bond, A. M.; Colton, R.; Lumscombe, D. L.; Moir, J. E. *J. Am. Chem. Soc.* **1986**, *108*, 3352. (b) Pickett, C. J.; Pletcher, D. *J. Chem. Soc., Dalton Trans.* **1975**, 879. (c) Klinger, R. J.; Kochi, J. K. *J. Am. Chem. Soc.* **1980**, *102*, 4790.

Table XIV. CO Stretching Frequencies of $Cp(1\text{-}R_3P\text{-}2,4\text{-}C_7H_{11})CrCO^+$ and of Its Phosphine Adducts in CH_2Cl_2

complex	ν_{CO}, cm^{-1}	ligand	ν_{CO}, cm^{-1} (adduct)
^{13}CO	1972	$P(n\text{-}Bu)_3$	1877
		PCy_3	1874
CO	2015	$P(n\text{-}Bu)_3$	1915
		PMe_2Ph	1913
		$PMePh_2$	1914
		PCy_3	1914
		PEt_3	1911

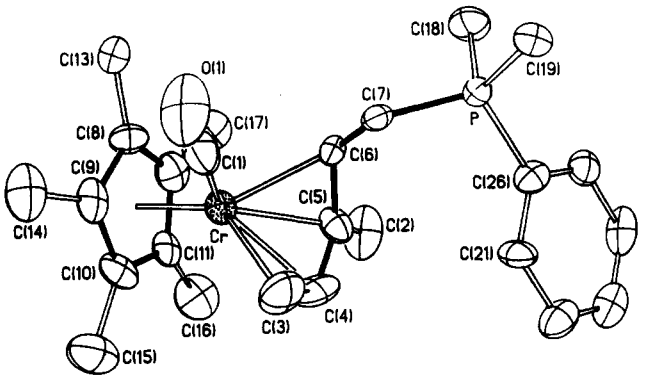

Figure 6. Molecular structure of $Cp^*(1\text{-}PMe_2Ph\text{-}3\text{-}C_6H_9)CrCO^+$.

electronic structure. In contrast, much has been learned about $V(CO)_6$. It is well accepted that CO substitution for $V(CO)_6$ occurs initially by attack of the entering ligand at the half-filled orbital, which in the metallocene carbonyl complexes is more shielded from biomolecular attack.[18]

Reactions of the 17-Electron Complexes with Strong Bases. Addition of $P(n\text{-}Bu)_3$ or other phosphine ligands (Table XII) to a solution of $[Cp(2,4\text{-}Me_2Pdl)CrCO]^+[BF_4]^-$ in dichloromethane or 1,2-dichloroethane leads to an immediate color change from red to green, disappearance of the CO band at 2015 cm^{-1}, and appearance of a new band around 1914 cm^{-1} (Table XIV). Similar behavior is seen for $Cp^*(3\text{-}C_6H_9)Cr(CO)^+$. ESR data for these products are included in Table XI. Although such nucleophilic additions to coordinated π-hydrocarbons are well-known,[19] we were surprised to see that small changes in basicities of the nucleophiles result in different reactions. Furthermore, the role which is defined for 18-electron complexes,[20] that nucleophilic attack occurs preferentially at the terminal carbon atom of an open π-hydrocarbon (vide infra), still applies to these 17-electron complexes. Notably, when purified red-brown $[Cp^*(1\text{-}PMe_2Ph\text{-}3\text{-}C_6H_9)Cr(CO)]^+[BF_4]^-$ was dissolved in CH_2Cl_2, a fast reverse reaction was observed. It appears in this case that there is a fast, reversible reaction in solution (eq 8).

$$Cp^*(3\text{-MePdl})Cr(CO)^+ + PR_3 \rightleftharpoons Cp^*(1\text{-}PR_3\text{-}3\text{-MePdl})Cr(CO)^+ \quad (8)$$

The weaker binding of PR_3 by the Cp* complex may easily be rationalized by either steric or electronic arguments. However, the situation actually appears more complex, as the cation colors are quite different, and analytical and ESR data for the green complex suggest an entirely different formulation. Apparently, the presence of the bulky, electron-donating Cp* group prevents more complex reactions from following the initial nucleophilic addition.

Figure 7. ESR spectrum of $Cp^*(1\text{-}PMe_2Ph\text{-}3\text{-}C_6H_9)CrCO^+$ in CH_2Cl_2 at room temperature.

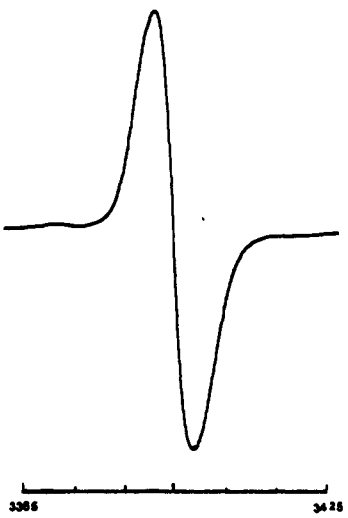

Figure 8. ESR spectrum of $Cp(1\text{-}PMe_2Ph\text{-}2,4\text{-}C_7H_{11})CrCO^+$ in CH_2Cl_2 at room temperature.

Table XV. Rate Constants and Activation Parameters for CO Dissociation from the PMe_2Ph Adduct of $Cp(2,4\text{-}C_7H_{11})CrCO^+$ in THF Solution

T, °C	k_1, s^{-1}	ΔH^*, kcal/mol	ΔS^*, cal/(mol·K)
31.6	2.37×10^{-5}	23.0 ± 1.4	−4.3 ± 4.5
40.1	7.61×10^{-5}		
48.8	19.0×10^{-5}		

An X-ray molecular structure determination was carried out on $[Cp^*(1\text{-}PMe_2Ph\text{-}3\text{-}C_6H_9)CrCO]^+[BF_4]^-$. The results show that PMe_2Ph is attached to a terminal carbon atom of the 3-MePdl ligand (Figure 6, Tables IV and V). While few reliable comparisons may be made for these structural data, it can be noted that the Cr–CO distance here (1.817 (11) Å) seems to be shorter than that in $Cp^*(3\text{-}C_6H_9)Cr(CO)^+$ (1.858 (7) Å).

The isolation of the PMe_2Ph adducts raises yet another question regarding CO substitution with RNC. The weak base ligands might first attack at the terminal carbon atom of Pdl, and then the CO substitution occurs by association mechanism or by ligand migration from Pdl to the metal. Both of these mechanisms agree with the observed second-order rate law. To test these possible mechanisms, kinetic studies on the loss of CO from the PMe_2Ph adducts have been carried out in THF solvent. The ESR spectra of the kinetic products do not show phosphorus spin

(18) Kowaleski, R. M.; Basolo, F.; Osborne, J. H.; Trogler, W. C. *Organometallics* **1988**, *7*, 1425.
(19) Kane-Maguire, L. A. P.; Honig, E. D.; Sweigart, D. A. *Chem. Rev.* **1984**, *84*, 525.
(20) Davies, S. G.; Green, M. L. H.; Mingos, D. M. P. *Tetrahedron* **1978**, *34*, 3047.

coupling (Figures 7 and 8), and the rates of disappearance of the carbonyl complexes are first-order in complex concentrations. A plot of ln (k/T) vs $1/T$ permits an estimate of activation parameters (Table XV).

The $\Delta H^{\ddagger}$ value (23.0 kcal/mol) is compatible with that for dissociation of CO from analogous complexes,[4,6] and the $\Delta S^{\ddagger}$ value is near zero (−4.3 cal/(mol·K)). These results are in accord with a dissociative mechanism (eq 9). The

$$\text{Cp*(1-PMe}_2\text{Ph-3-MePdl)Cr(CO)}^+ \underset{+\text{CO}}{\overset{k_1}{\underset{-\text{CO}}{\rightleftharpoons}}} \text{Cp*(1-PMe}_2\text{Ph-3-MePdl)Cr}^+ + \text{CO} \quad (9)$$

rate of the reaction was retarded by added CO, which is consistent with a dissociative equilibrium (Table XII). Although the final products were not isolated and characterized, they cannot be converted to the parent complex under a CO atmosphere (1 atm). These results imply that CO substitution does not first take place by RNC attack on the pentadienyl followed by RNC transfer to the metal but rather by direct nucleophilic attack of RNC at the metal center. Since no RNC adduct was observed, K would be $\ll 1$ for the equilibria reactions (eq 8), when RNC is the nucleophile. Thus, if CO substitution were to follow the addition of RNC on the terminal carbon of Pdl (eq 8), then at 40 °C $k_2 = Kk_1 = (7 \times 10^{-5})K \ll 7 \times 10^{-5}$ (Table XV). This is in contrast to the experimental results, which show that $k_2 = 2 \times 10^{-4}$ (Table X). Compared with the parent complexes, addition of phosphine ligand to Pdl promotes dissociation of the CO ligand from the metal, despite the values of ν_{CO} which show there is stronger π-back-bonding from the metal to CO in the adducts.

Conclusions

The one-electron oxidations of Cp(Pdl)Cr(CO) compounds to the 17-electron cations lead to a rearrangement of the Pdl coordination from η^5(S) (sickle) to η^5(U). Dissociative exchange between coordinated and free CO for the cations is extremely slow. Reactions with isocyanide ligands followed different pathways, in which the Pdl ligands were lost, and species such as $CpCr(CNR)_4^+$ were formed. The addition of phosphines to the cations generally seemed to lead to a nucleophilic attack on a terminal carbon atom of the pentadienyl ligand, leading essentially to a 17-electron Cp(η^4-diene-PR_3^+)Cr(CO) species from $[Cp^*(3\text{-}C_6H_9)Cr(CO)]^+$ and an even more unusual species from $Cp(2,4\text{-}C_7H_{11})Cr(CO)^+$, yet to be conclusively characterized.

Acknowledgment. We express our appreciation for generous support of this research by the National Science Foundation and by our universities.

Supplementary Material Available: Pertinent bonding, positional, and thermal parameter tables for $[Cp(2,4\text{-}C_7H_{11})Cr(CO)]^+I^-\cdot CH_3CN$, anisotropic thermal parameter, H atom positional parameter, and least-squares plane tables for $[Cp^*(3\text{-}C_6H_9)Cr(CO)]^+[BF_4]^-$, crystallographic data and data collection and refinement detail, isotropic and anisotropic thermal parameter, bond distance and angle, and H atom positional parameter tables for $[CpCr(CN\text{-}t\text{-}C_4H_9)_4]^+[CpCr(CO)_3]^-$ and $[CpCr(CN\text{-}t\text{-}C_4H_9)_4]^+[BF_4]^-$, crystallographic data and data collection and refinement detail and isotropic and anisotropic thermal parameter tables for $[Cp^*(1\text{-}PMe_2Ph\text{-}3\text{-}C_6H_9)Cr(CO)]^+[BF_4]^-$ and a diagram of $[CpCr(CN\text{-}t\text{-}C_4H_9)_4]^+[BF_4]^-$ (27 pages). Ordering information is given on any current masthead page.

OM920105D

Observation of Rhodocenium and Substituted-Rhodocenium Ions and Their Neutral Counterparts by Mass Spectrometry

Dmitri V. Zagorevskii* and John L. Holmes*

Chemistry Department, University of Ottawa, Ottawa, Ontario, Canada K1N 6N5

Received February 20, 1992

Ionized rhodocene and its hydroxymethyl and carboxyl derivatives have been generated in the gas phase and characterized by tandem mass spectrometry. The fragmentations of these ions resemble the decomposition pathways for corresponding ferrocenium, but Cp_2Rh^+ ions show greater dehydrogenation and ligand(s) decomposition processes. Substituent decomposition reactions dominate in the case of (hydroxymethyl)- and carboxyrhodocenium. Neutralization–reionization experiments showed the existence of neutral rhodocene and rhodocenecarboxylic acid as stable species in the gas phase.

Introduction

One of the more interesting compounds among the bis(cyclopentadienyl) complexes of transition metals, Cp_2M, is rhodocene (M = Rh). This 19-electron radical complex was observed when its stable 18-electron analogue[1] was electrochemically reduced, and the estimated half-life of Cp_2Rh was measured to be ca. 2 s in acetonitrile solution at 25 °C.[2] A method for stabilizing both rhodocene and rhodocenium derivatives is to insert substituents into the cyclopentadienyl ligand(s) in order to delocalize positive charge or electron density and to create steric hindrance to the attack of intra reagents on the metal atom. This is a likely reason for the richer chemistry of polysubstituted rhodocenium compared with the chemistry of mono- or disubstituted complexes.[3] For monosubstituted rhodo-

(1) (a) Cotton, F. A.; Whipple, R. O.; Wilkinson, G. *J. Am. Chem. Soc.* **1953**, *75*, 3586. (b) Birmingham, J. M.; Fischer, A. K.; Wilkinson, G. *Naturwissenschaften* **1955**, *42*, 96.

(2) El Murr, N.; Sheats, J. E.; Geiger, W. E., Jr.; Holloway, J. D. L. *Inorg. Chem.* **1979**, *18*, 1443.

0276-7333/92/2311-3224$03.00/0